Title

Tumor-Infiltrating Regulatory T Cells Inhibit Endogenous Cytotoxic T Cell Responses to Lung Adenocarcinoma

Journal

The Journal of Immunology, 191(4)

ISSN

0022-1767

Authors

Ganesan, Anusha-Preethi
Johansson, Magnus
Ruffell, Brian
et al.

Publication Date

2013-08-15

DOI

10.4049/jimmunol.1301317

Peer reviewed

Published in final edited form as:
J Immunol. 2013 August 15; 191(4): 2009–2017. doi:10.4049/jimmunol.1301317.

Tumor-infiltrating regulatory T cells inhibit endogenous cytotoxic T cell responses to lung adenocarcinoma

Anusha-Preethi Ganesan[*,§], **Magnus Johansson**[*], **Brian Ruffell**[*,¶], **Adam Beltran**[†,‡], **Jonathan Lau**[*], **David M. Jablons**[*,‡], and **Lisa M. Coussens**[*,†,¶,‖]

[*]Department of Pathology, University of California, San Francisco, San Francisco, CA 94143, USA

[†]Helen Diller Family Comprehensive Cancer Center, University of California, San Francisco, San Francisco, CA 94143, USA

[‡]Department of Surgery, University of California, San Francisco, San Francisco, CA 94143, USA

[§]Cancer Sciences Division, University of Southampton, Tremona Road, Southampton SO16 6YD, UK

Abstract

Immune cells comprise a substantial proportion of the tumor mass in human non-small cell lung cancers (NSCLC), but the precise composition and significance of this infiltration is unclear. Herein we examined immune complexity of human NSCLC as well as NSCLC developing in CC10-TAg transgenic mice, and revealed that $CD4^+$ T lymphocytes represent the dominant population of $CD45^+$ immune cells, and relative to normal lung tissue, $CD4^+FoxP3^+$ regulatory T cells (T_{regs}) were significantly increased as a proportion of total $CD4^+$ cells. To assess the functional significance of increased T_{reg} cells, we evaluated $CD8^+$ T cell-deficient/CC10-TAg mice and revealed that $CD8^+$ T cells significantly controlled tumor growth with anti-tumor activity that was partially repressed by T_{reg} cells. However, while treatment with anti-CD25 depleting mAb as monotherapy preferentially depleted T_{regs} and improved $CD8^+$ T cell-mediated control of tumor progression during early tumor development, similar monotherapy was ineffective at later stages. Since mice bearing early NSCLC treated with anti-CD25 mAb exhibited increased tumor cell death associated with infiltration by $CD8^+$ T cells expressing elevated levels of granzyme A, granzyme B, perforin and interferon-γ, we therefore evaluated carboplatin combination therapy resulting in a significantly extended survival beyond that observed with chemotherapy alone, indicating that T_{reg} depletion in combination with cytotoxic therapy may be beneficial as a treatment strategy for advanced NSCLC.

Classification

Lung; Tumor Immunity; T cells; Rodent; Human

[‖]Address for correspondence: Lisa M. Coussens, Ph.D., Cell & Developmental Biology, Knight Cancer Institute, Oregon Health & Science University, Mail Code L215, 3181 SW Sam Jackson Park Road, Portland, OR 97239-3098, Voice: 503-494-7811, Fax: 503-494-4253, coussenl@ohsu.edu.
[¶]Current address: Department of Cell and Developmental Biology, Knight Cancer Institute, Oregon Health and Science University, Portland, OR 97239

INTRODUCTION

Lung cancer is the most common cause of cancer-related mortality worldwide, with approximately 85% being of the non-small cell (NSCLC) histological subtype, and associated with prior tobacco use (1). Despite advances in treatment modalities, survival rates for advanced lung cancer remain poor, thus innovative therapeutic approaches are urgently needed.

Retrospective analysis of most human tumors (2), including lung (3–7), have revealed a significant correlation between immune infiltration by $CD8^+$ cytotoxic T cells and improved outcome. In contrast, infiltration of tumors by regulatory T cells (T_{regs}) expressing the lineage-specific transcription factor FoxP3 is instead associated with poor prognosis in NSCLC and other carcinomas (8–12). As T_{regs} are thought to function primarily in cancer by repressing $CD8^+$ T cell functionality, the reciprocal relationship between these two immune cell subtypes indicates that depleting T_{regs} might be therapeutically beneficial.

Indeed, several studies employing carcinogen-induced or transplantable tumor models have reported therapeutic efficacy by depleting T_{regs} based upon increased expression of the interleukin-2 receptor CD25 (13). However, tumors arise spontaneously following an initiating mutation and not by sudden introduction of fully transformed cells, or by high-dose, short period carcinogen exposure. Furthermore, therapeutic efficacy in these studies was only observed when depletion was performed prior to tumor cell inoculation or cancer initiation, making translation of these findings to the clinic difficult.

As the tumor immune microenvironment and the immunosuppressive cell types that function in tissues are distinct, we first evaluated leukocyte complexity of human NSCLC and found that $CD4^+$ T cells were significantly increased relative to adjacent normal lung tissue, and that $CD4^+Foxp3^+T_{regs}$ constituted a significant proportion of these tumor-infiltrating cells. To determine the functional significance of these adaptive leukocytes, and the cellular and molecular mediators of pro- versus anti-tumor immunity, we utilized a transgenic mouse model of multistage lung carcinogenesis, namely CC10-TAg mice, in which SV40 T antigen driven carcinogenesis mirrors that of aggressive human lung cancers (14). We revealed that while $CD8^+$ T lymphocytes are critical in restraining lung tumor growth, their recruitment into tumors and bioeffector functions are inhibited by $CD4^+Foxp3^+T_{regs}$, depletion of which significantly prolongs survival of tumor-bearing mice in combination with chemotherapy (CTX).

MATERIALS AND METHODS

Human tissue samples

Patients with non-small cell lung cancer who had not received neo-adjuvant therapy were recruited into the study under approval of local Institutional Review Boards. Informed written consent was obtained from the patients. Tumor tissue, adjacent normal tissue and blood were collected from patients following surgical resection at UCSF and histo-pathological diagnosis was obtained at the same center.

Animal studies

Generation of CC10-TAg mice and characterization of their neoplastic/histopathological stages have been previously reported (15). CC10-TAg mice deficient in B cells ($JH^{-/-}$), $CD4^+$ T cells ($CD4^{-/-}$), $CD8^+$ T cells ($CD8^{-/-}$) and both $CD4^+$ and $CD8^+$ T cells ($CD4^{+/-}CD8^{+/-}$) were generated by backcrossing $JH^{+/-}$, $CD4^{+/-}$, $CD8^{+/-}$ and $CD4^{+/-}CD8^{+/-}$ mice respectively into the FvB/n strain to at least N5 (16, 17) followed by intercrossing with CC10-TAg mice. All animal studies and procedures conformed to

National Institute of Health guidelines and were approved by UCSF Institutional Animal Care and Use Committee (IACUC). For *in vivo* depletion studies, mice were injected intra-peritoneally with 400 μg of αCD25 mAb (Clone PC61) and 500 μg of αCD8 mAb (Clone YTS169.4) every 5 days for the respective time periods as indicated. For survival studies, mice were treated with 400 μg αCD25 mAb (Clone PC61) or isotype control from 8 weeks of age until end-stage defined by 15% weight loss. Carboplatin (Hospira) was injected intra-peritoneally at 50 mg/kg every 5 days for 3 doses starting at 13 weeks of age.

Histology and tumor size

Mice were sacrificed at indicated time-points and all tissues were collected following intra-cardiac PBS perfusion. Tissues were fixed in 10% neutral-buffered formalin or frozen in OCT. Tumor burden of each mouse was quantified in five H&E stained serial sections (100 μm apart) of lungs using Image J software.

Immunohistochemistry

5 μm sections of formalin-fixed paraffin embedded (FFPE) tissues were de-paraffinised in xylene and rehydrated by immersion in reducing concentrations of alcohol followed by PBS. Antigen retrieval for CD45, CD8, Foxp3, cleaved caspase-3 and BrdU staining was performed by boiling in citrate buffer (BioGenex), followed by incubation with proteinase K (Dako) for CD31. Endogenous peroxidase activity was quenched by incubation in hydrogen peroxide (Sigma) and methanol at 1:50. Following blocking of non-specific binding by application of blocking buffer (PBS containing 5% goat serum, 2.5% bovine serum albumin and 0.1% Tween 20), tissue sections were incubated overnight with primary antibodies, e.g., CD8 (Novus Biolabs), Foxp3 (eBioscience), cleaved caspase-3 (Cell Signaling), BrdU (AbD Serotec), CD45 (BD Bioscience) and CD31 (BD Bioscience) at 4° C. After washing in PBS, tissue sections were incubated with their respective biotinylated secondary antibodies for 30 minutes at room temperature followed by horseradish peroxidase-conjugated avidin complex (ABC Elite, Vector Laboratories). Tissue sections were finally developed with 3,3 diaminobenzidine (DAB, Vector Laboratories), counterstained with methyl green, dehydrated and mounted with Cytoseal (Thermo Scientific). Slides were digitally scanned by Aperio ScanScope CS Slide Scanner to generate images and quantification of positive staining was performed using Aperio algorithms.

Flow cytometry

Human and murine lung tissues were sliced and digested using collagenase A (Roche), elastase (Worthington Biochemicals) and DNase (Roche) at 37°C for 20 minutes. Enzyme activity was quenched by addition of fetal calf serum (Sigma) and resulting single cell suspension filtered through a 100 μm filter (BD Bioscience). Cells were washed in DMEM (Invitrogen) supplemented with 10% fetal calf serum followed by lysis of erythrocytes (RBCs) by incubation with lysis buffer (BD Bioscience) on ice for 10 minutes. Live cells were then counted using trypan blue staining with a hemocytometer. Non-specific antibody binding was blocked by incubation of cells with Fc Receptor Binding Inhibitor (eBioscience) on ice for 30 minutes, followed by labeling with Fixable Live/Dead Aqua (invitrogen) and fluorophore-conjugated primary antibodies as has been previously described for human (18) and mouse (19). Cells were washed in PBS containing 1.0% BSA and fixed using BD Cytofix (BD Bioscience) for 30 minutes followed by a further wash and stored at 4°C until analysis. Intracellular staining for Foxp3 was performed using Foxp3 Staining Kit (eBioscience) as per the manufacturer's recommendations. Briefly, following labeling with fluorophore-conjugated primary antibodies, cells were fixed using the Fixation/Permeabilization Buffer (eBioscience) and the washed with Permeabilization Buffer (eBioscience). Cells were incubated with fluorophore-conjugated anti-Foxp3

antibody and further washed using Permeabilization Buffer (eBioscience). All samples were analyzed on an LSRII flow cytometer (BD Bioscience).

qPCR assays

mRNA was obtained by processing tissue samples as per recommendations using RNeasy Micro/Mini Kit (Qiagen) and quantified with NanoDrop ND-1000 (Thermo Fisher Scientific). cDNA was prepared from mRNA by reverse transcription suing Superscript III. Pre-amplification of cDNA for genes of interest was performed using TaqMan PreAmp Master Mix Kit (Applied Biosystems). PCR amplification to 40 cycles was performed using TaqMan Gene Expression Assays (Applied Biosystems) for respective genes and TaqMan Gene Expression Master Mix (Applied Biosystems) in 20 μl reactions at recommended cycle temperature conditions on an ABI 7900HT quantitative PCR machine (ABI Biosystems). Differences in gene expression was determined by calculating relative expression as fold change over *TBP* used as the house keeping gene.

Statistical analyses

Statistical analyses were performed using Prism 4.0 (GraphPad Software). Differences between groups for all parameters was determined using Mann-Whitney Test (unpaired, non-parametric, two-tailed) except for survival studies where Log Rank Test was used. $*p<0.05$; $**p<0.01$, $***p<0.001$ is shown for all figures.

RESULTS

Human non-small cell lung cancers are infiltrated by $CD4^+$ T and B lymphocytes

Using immunohistochemical and flow cytometric approaches, we evaluated the immune microenvironment within tumors of patients with CTX-naive NSCLC (Table S1), and found increased presence of $CD45^+$ leukocytes within tumors as compared to adjacent normal tissue (Fig. 1A–B). Both adaptive lineage (T and B lymphocytes) and innate lineage cells (macrophages, dendritic cells and granulocytes) were observed in normal adjacent lung and tumor tissue. However, as compared to adjacent normal lung tissue, the relative composition of leukocytes within tumors was skewed towards higher proportions of $CD4^+$ T and B cells (Fig. 1C–D). In all of the tumors examined both $CD4^+$ and $CD8^+$ T cells displayed activated phenotypes, with most samples displaying higher percentage of $CD69^+$ cells in tumors as compared to normal adjacent tissue (Fig. 1E).

Immune complexity of CC10-TAg NSCLCs mirrors human NSCLC

CC10-TAg mice express the Simian virus 40 large T antigen under control of the Clara cell promoter, and as a consequence develop multifocal pulmonary adenocarcinoma (15) with a gene signature correlated with that of aggressive subtypes of human lung cancers, and thus represent a relevant preclinical model to study NSCLC development (14). In CCT10-TAg mice, hyperplastic and dysplastic lung tissue is prominent as early as 4 weeks of age, and develops into adenomas by 8 weeks, with invasive NSCLC in 100 percent of mice on the FVB/n strain background between 12 and 16 weeks of age (15). Similar to human NSCLC, CC10-TAg tumors are characterized by marked $CD45^+$ leukocytic infiltration (Fig. 2A–B) with an increased percent of $CD4^+$ T lymphocytes (Fig. 2C–D).

Endogenous $CD8^+$ cytotoxic T cell responses restrain lung tumor growth in CC10-TAg mice

Since our data indicated that human NSCLCs were predominantly infiltrated by activated T lymphocytes, we investigated the functional significance of $CD4^+$ T, $CD8^+$ T and B cells in CC10-TAg mice by generating mice harboring homozygous null mutations in genes

controlling lineage development. CC10-TAg mice deficient for $B220^+CD19^+$ mature B cells (CC10-TAg/$JH^{-/-}$), $CD4^+$ T cells (CC10-TAg/$CD4^{-/-}$), $CD8^+$ T cells (CC10-TAg/$CD8^{-/-}$), and mice lacking both $CD4^+$ and $CD8^+$ T cells (CC10-TAg/$CD4^{-/-}CD8^{-/-}$) were evaluated for tumor burden at 12 weeks of age. CC10-TAg mice lacking $CD8^+$ T cells, but not $CD4^+$ T cells or B cells, exhibited increased tumor burden (Fig. 3A–B), accelerated progression to end-stage, and reduced survival (Fig. 3C); indicating that endogenous $CD8^+$ T cell responses played a critical role in limiting tumor growth and progression. To demonstrate that the phenotype of CC10-TAg/$CD8^{-/-}$ mice was not a side effect of genetic manipulation, we depleted $CD8^+$ T cells from CC10-TAg mice from 8 weeks to 12 weeks of age using αCD8 depleting antibodies that efficiently depleted $CD8^+$ T cells in both spleen and lungs (Fig. S1A). Antibody-mediated depletion phenocopied the CC10-TAg/$CD8^{-/-}$ mice (Fig. 3D), thereby demonstrating that $CD8^+$ T cells were functionally important in restraining tumor growth in the CC10-TAg model.

Human and CC10-TAg lung tumors are infiltrated by $CD4^+Foxp3^+$ T regulatory cells

$CD8^+$ cytotoxic T cells infiltrate lung tumors where they functionally regulate tumor growth; nevertheless, CC10-TAg tumors continue to progress with mice eventually succumbing to respiratory insufficiency. Given that $CD4^+$ T cells abundantly infiltrate tumors relative to non-tumor bearing lungs, we hypothesized that $Foxp3^+$ T_{regs} might be enriched within tumors where they functioned to suppress productive $CD8^+$ T cell responses. To investigate this, we first ascertained if T_{regs} were present in tumors by intracellular staining for Foxp3 by flow cytometry and immunohistochemistry. We observed that indeed within human NSCLC tumors (Fig. 4A), there was enrichment of $CD4^+$ $Foxp3^+$ T_{regs} relative to adjacent normal lung tissue. These findings were mirrored in CC10-TAg lung tumors at multiple stages of tumor development (Fig. 4B), where upregulation of CD103 surface expression in tumor infiltrating T_{regs}, as compared to normal lungs, was also observed and thus indicating their activated phenotype (Fig. 4C).

T regulatory cell depletion diminishes tumor burden in CC10-TAg mice

To examine the functional significance of T_{reg} infiltration of lung tumors, we examined the effects of partial T_{reg} depletion. Although complete and specific elimination of T_{regs} can be achieved by use of scurfy mice (20) harboring a loss-of-function mutation in the Foxp3 gene, or by administration of diphtheria toxin to $Foxp3^{DTR}$ mice (21), development of fatal autoimmunity early on in these mice precludes their use for long term tumor studies. We thus depleted T_{regs} using an anti-CD25 depleting mAB (αCD25; clone PC61) that depletes the major subset of $FoxP3^+$ T_{reg} cells expressing CD25, the high affinity IL-2 receptor α-chain.

Although T_{regs} are characterized by constitutive CD25 expression, CD25 can also be upregulated on conventional $CD4^+$ and $CD8^+$ T cells following activation. Hence we first determined the profile of cells expressing CD25 in lung tumors and observed that within CC10-TAg tumors, the majority of CD25 expressing T cells co-expressed FoxP3 (Fig. S1B). Administration of a single dose of the αCD25 mAb resulted in progressive diminution of T_{regs} in peripheral blood, attaining a maximum reduction of 70% as compared to control mice 5 days post-injection, with some evidence of recovery by day 11 (Fig. S1C).

Treatment of 4 week old CC10-TAg mice every 5 days with αCD25 mAb until mice were 8 weeks old (Fig. 5D) significantly reduced presence of T_{regs} within spleen and tumor-bearing lungs (Fig. 5E) and lead to a significant, albeit minor, reduction in tumor burden (Fig. 5F). This reduction in tumor burden was not due to reduced presence of proliferating malignant lung epithelia (Fig. 4G) or changes in vascular architecture (Fig. 4H), but instead by a marked increased presence of cleaved caspase-3-positive cells (Fig. 4I) that correlated with

increased presence of $CD8^+$ T cells infiltrating lung parenchyma and tumors (Fig. 4J–L). Together these data indicated that T_{regs} were likely involved in restricting anti-tumor activity of tumor-infiltrating $CD8^+$ T cells.

Enhanced recruitment of $CD8^+$ T cells restricts NSCLC development

Analysis of infiltrating $CD8^+$ T cells in T_{reg}-depleted CC10-TAg mice revealed no difference in *in vivo* proliferation as measured by BrdU incorporation (Fig. 5A) or activation as determined by CD69 expression (Fig. 5B). Instead, gene expression analysis of FACS-sorted $CD8^+$ T cells isolated from tumors revealed significantly enhanced expression of the T_H1 cytokine IFN-γ (Fig. 5C), and cytotoxic effector molecules granzyme A (Fig. 5D), granzyme B (Fig. 5E) and perforin (Fig. 5F). A functional role for $CD8^+$ T cells following T_{reg} depletion was confirmed using CC10-TAg/$CD8^{-/-}$ mice, where as expected αCD25 mAb administration from 4 to 8 weeks of age failed to alter tumor burden at end-stage (Fig. 5G).

As other studies have reported that T_{reg} suppression of effector T cells may be mediated by cross-talk with antigen presenting cells (22–25), we also examined whether $CD11c^+MHCII^+$ alveolar macrophage (Fig. S2) or $CD11c^{hi}MHCII^{hi}$ dendritic cell (DC) (Fig. S3) polarization might be altered following partial T_{reg} depletion. Although a significant reduction of CCL17 and CCL22, chemokines known to promote recruitment of T_{regs} into tumors, was observed in tumor-isolated $CD11c^+MHCII^+$ alveolar macrophages, baseline expression of these genes was 100-fold lower compared to DCs, which did not display altered gene expression. Hence we reasoned this was unlikely to account for changes in $CD8^+$ T cell activity. Based on the modest changes in macrophage and DC transcriptomes, we therefore speculated that T_{regs} were the major leukocyte population repressing $CD8^+$ T cell presence and effector function.

T regulatory cell depletion in combination with chemotherapy extends survival of CC10-TAg mice

Preclinical studies in murine models of cancer and early phase clinical trials have revealed limited success in extending survival when immunotherapeutic strategies employing T_{reg} depletion are administered as monotherapy for established tumors (26). Because T_{reg} depletion attenuated tumor burden in CC10-TAg mice in a prevention trial, we sought to evaluate whether T_{reg} depletion in combination with cytotoxic CTX might extend survival of CC10-TAg mice in a more clinically relevant setting when mice with late-stage NSCLC were treated. Since platinum compounds are first line ‘standard-of-care’ chemotherapeutic agents for human NSCLC, we first conducted dose-response experiments with cisplatin in CC10-TAg mice to determine the maximum tolerated dosage that would not produce total leucopenia for use in survival studies. We observed that 50% of CC10-TAg mice did not tolerate administration of both cisplatin and mAb despite the reported safety profile of combinatorial cisplatin and mAbs in clinical trials (27, 28). We therefore conducted a similar dose-response study with carboplatin, and determined the maximum tolerated dose in combination with α-CD25 mAb to be 50 mg/Kg, with peripheral blood erythrocytes, leukocytes (lymphocytes and granulocytes) and platelets showing reduced, but not abnormal levels in mice (data not shown).

Thus, CC10-TAg mice were randomized and recruited into four arms to evaluate survival. Mice received control IgG or αCD25 mAb as monotherapy from 8 weeks of age until end-stage (15% weight loss), or received mAbs in combination with carboplatin CTX administered in 3 doses, 5 days apart, commencing at 13 weeks when CC10-TAg mice histopathologically exhibit features of invasive adenocarcinomas. While administration of αCD25 mAb as a monotherapy yielded no survival benefit as compared to control IgG-

treated mice, mice that received combination αCD25 mAb plus carboplatin exhibited a significant ($p<0.05$) extension of survival relative to carboplatin alone (Fig. 6).

DISCUSSION

Herein, we evaluated leukocyte complexity of human NSCLC from CTX-naive patients and in a mouse model of de novo NSCLC development. Results from these studies indicates that while lymphocytes and myeloid cells infiltrate both NSCLC and normal lung, the immune complexity of human NSCLC is dominated by T cells and in particular, $CD4^+$ T and B cells as compared to adjacent normal lung tissue. Interestingly in over half of the patient tissues examined, both $CD4^+$ and $CD8^+$ tumor-infiltrating T cells, exhibited an activated phenotype based upon expression of CD69, as compared to those in adjacent normal tissue, indicating that these lymphocytes may be functionally significant. $CD4^+$ T cells can protect against methylcholanthrene-induced sarcomas (29) and human papilomavirus type (HPV16)-induced cervical carcinogenesis (30), while in other tissues instead promote carcinogen-induced (31) or human papillomavirus (HPV)16-induced squamous cancer (32). In a similar manner, B cells have been found to dampen anti-tumor immune responses in some murine tumors (33, 34), while augmenting them to enable tumor rejection in others. (35, 36). It has therefore become increasingly clear that tumor-infiltrating immune cells exert different bioactivities depending on context, namely tumor etiology and tumor microenvironment.

In CC10-TAg mice harboring NSCLC, neither $CD4^+$ T cell or B cell-deficiency significantly altered tumor growth or progression; in contrast, $CD8^+$ T cell-deficiency led to an acceleration of tumor growth and reduction in survival, thus indicating their critical role in thwarting tumor development in lung. Nevertheless, all CC10-TAg mice succumbed to their disease indicating tumor immune escape. In keeping with previous reports (37, 38) we found enhanced T cell infiltration in both human and murine NSCLCs relative to normal adjacent or nontransgenic lung, respectively. If $CD4^+Foxp3^+T_{regs}$ infiltrating NSCLC were functionally significant in promoting tumor immune escape in NSCLC, the expectation would instead be tumor regression in $CD4^+$ T cell-deficient CC10-Tag mice, a result that was not observed. However the conflict in our observation may be accounted for by the simultaneous absence of conventional $CD4^+$ T cells in CD4-deficient TAg mice, which may be essential for providing 'help' to $CD8^+$ T cells (39, 40).

The functional significance of T_{regs} in several malignancies has been elucidated using mouse models (41–45), however their precise role in lung cancer is unclear. Further, the *in vivo* mechanism, the target cell-types and molecular mediators utilized by T_{regs} to exert their suppressive function in the tumor microenvironment are incompletely understood. Herein, we report that in CC10-TAg mice, depletion of T_{regs} using the αCD25 mAb (PC61) at an early stage of tumor development significantly reduced tumor burden in a manner dependent upon infiltration of functionally active $CD8^+$ T cells. Tumor-infiltrating $CD8^+$ T cells in T_{reg}-depleted mice did not display enhanced activation or *in vivo* proliferation, indicating that increased $CD8^+$ T cell infiltration observed following T_{reg} depletion was likely a result of increased recruitment rather than local proliferation. That said, $CD8^+$ T cells infiltrating tumors of T_{reg}-depleted mice were characterized by upregulation of effector cytotoxic genes, including granzyme A, granzyme B and perforin, indicating enhanced functional capacity following release from T_{reg}-mediated suppression. Taken together, these findings indicate that $CD8^+$ T cells recruited to NSCLCs following T_{reg} depletion were functionally empowered to better kill malignant cells (as indicated by increased presence of cleaved caspase-3 cells) leading to increased tumor cell death. Our data implicating T_{reg} suppression of $CD8^+$ T cells is supported by several studies (41, 42) although other cell types, such as conventional $CD4^+$ T cells and natural killer (NK), have also been reported to be involved (46, 47). Unexpectedly, a recent study by Teng and colleagues revealed a requirement for

T_H2 cytokines, interleukin (IL)-4 and IL-13 in addition to the T_H1 cytokine IFN-γ in achieving tumor control following T_{reg} depletion using respective cytokine-deficient mice (48).

T_{regs} regulate antigen-presenting cell (APC) function as a means of regulating immune responses. T_{regs} establish direct interactions with DCs in lymph nodes leading to impaired ability to engage and activate T effector cells (49). T_{reg} modulation of macrophages also results in reduced activation, blunted pro-inflammatory cytokine secretion, upregulation of CD206 and CD163, and reduced macrophage cytotoxicity (50, 51). Both DCs and macrophages can be stimulated by T_{regs} to produce immunosuppressive molecules such as IDO, IL-10 and TGF-β (22, 25, 52). We assessed whether T_{regs} exerted their suppressive effect on APCs in the lung tumor microenvironment and found no significant changes in either DC or macrophage gene expression profiles when comparing T_{reg}-depleted NSCLC versus and control NSCLC tissue, indicating that T_{regs} likely directly suppress $CD8^+$ T cells in the lung.

Prophylactic T_{reg} depletion in many experimental murine cancer models results in tumor protection when T_{regs} depletion precedes tumor cell implantation (41, 43, 53, 54). In contrast, T_{regs} depletion as monotherapy in large established tumors exhibits minimal impact (26). Recent studies have also revealed that conventional CTX causes tumor regression not just by direct tumor cell killing, but also by eliciting an anti-tumor cytotoxic immune response (55). Thus, we hypothesized that depletion of T_{regs} in combination with CTX would exert synergistic effects in restraining established tumors. Indeed we revealed that CC10-TAg mice display enhanced survival when treated with a combination of αCD25 mAb and carboplatin, as compared to either treatment alone. This study thus highlights that even in established tumors, manipulation of T_{regs} may be beneficial in combination with ‘standard-of-care’ conventional CTX. Survival benefits have also been reported for early treatment of implanted mesothelioma tumors using αCD25 mAb and pemetrexed (56). Interestingly, two other reports revealed that complete and selective T_{reg} depletion using DEREG mice controls growth of established implanted tumors in isolation (57) or in combination with vaccination (58). As T_{reg} cells from transgenic murine tumors have been described to derive from the thymus (59), it will be interesting to determine whether this is also true for implantable tumor models, and whether these cells are functionally equivalent.

Supplementary Material

Refer to Web version on PubMed Central for supplementary material.

Acknowledgments

We acknowledge Drs. David G. DeNardo, Nesrine Affara, Stephen Shiao and Collin Blakely for helpful discussions, and Lidiya Korets and Kerri Fujikawa for technical assistance with maintenance of animals.

Funding: The authors acknowledge support from Cancer Research UK (CRUK) to APG, the Department of Defense Breast Cancer Research Program (BCRP) to BR, and grants from the NIH/NCI (R01 CA130980, R01CA140943, R01 CA155331, U54 CA163123), the Department of Defense BCRP Era of Hope Scholar Expansion Award (BC10412), the Susan G Komen Foundation (KG111084, KG110560), the Breast Cancer Research Foundation to LMC, and NIH/NCI R01 CA132566 to DMJ and LMC.

REFERENCES

1. Jemal A, Bray F, Center MM, Ferlay J, Ward E, Forman D. Global cancer statistics. CA Cancer J Clin.
2. Fridman WH, Pages F, Sautes-Fridman C, Galon J. The immune contexture in human tumours: impact on clinical outcome. Nat Rev Cancer. 2012; 12:298–306. [PubMed: 22419253]

3. Johnson SK, Kerr KM, Chapman AD, Kennedy MM, King G, Cockburn JS, Jeffrey RR. Immune cell infiltrates and prognosis in primary carcinoma of the lung. Lung Cancer. 2000; 27:27–35. [PubMed: 10672781]
4. Donnem T, Al-Shibli K, Andersen S, Al-Saad S, Busund LT, Bremnes RM. Combination of low vascular endothelial growth factor A (VEGF-A)/VEGF receptor 2 expression and high lymphocyte infiltration is a strong and independent favorable prognostic factor in patients with nonsmall cell lung cancer. Cancer. 116:4318–4325. [PubMed: 20549821]
5. Al-Shibli KI, Donnem T, Al-Saad S, Persson M, Bremnes RM, Busund LT. Prognostic effect of epithelial and stromal lymphocyte infiltration in non-small cell lung cancer. Clin Cancer Res. 2008; 14:5220–5227. [PubMed: 18698040]
6. Welsh TJ, Green RH, Richardson D, Waller DA, O'Byrne KJ, Bradding P. Macrophage and mast-cell invasion of tumor cell islets confers a marked survival advantage in non-small-cell lung cancer. J Clin Oncol. 2005; 23:8959–8967. [PubMed: 16219934]
7. Kawai O, Ishii G, Kubota K, Murata Y, Naito Y, Mizuno T, Aokage K, Saijo N, Nishiwaki Y, Gemma A, Kudoh S, Ochiai A. Predominant infiltration of macrophages and CD8(+) T Cells in cancer nests is a significant predictor of survival in stage IV nonsmall cell lung cancer. Cancer. 2008; 113:1387–1395. [PubMed: 18671239]
8. Curiel TJ, Coukos G, Zou L, Alvarez X, Cheng P, Mottram P, Evdemon-Hogan M, Conejo-Garcia JR, Zhang L, Burow M, Zhu Y, Wei S, Kryczek I, Daniel B, Gordon A, Myers L, Lackner A, Disis ML, Knutson KL, Chen L, Zou W. Specific recruitment of regulatory T cells in ovarian carcinoma fosters immune privilege and predicts reduced survival. Nat Med. 2004; 10:942–949. [PubMed: 15322536]
9. Bates GJ, Fox SB, Han C, Leek RD, Garcia JF, Harris AL, Banham AH. Quantification of regulatory T cells enables the identification of high-risk breast cancer patients and those at risk of late relapse. J Clin Oncol. 2006; 24:5373–5380. [PubMed: 17135638]
10. Shen Z, Zhou S, Wang Y, Li RL, Zhong C, Liang C, Sun Y. Higher intratumoral infiltrated Foxp3+ Treg numbers and Foxp3+/CD8+ ratio are associated with adverse prognosis in resectable gastric cancer. J Cancer Res Clin Oncol. 136:1585–1595. [PubMed: 20221835]
11. Zhou J, Ding T, Pan W, Zhu LY, Li L, Zheng L. Increased intratumoral regulatory T cells are related to intratumoral macrophages and poor prognosis in hepatocellular carcinoma patients. Int J Cancer. 2009; 125:1640–1648. [PubMed: 19569243]
12. Ruffell B, Denardo DG, Affara NI, Coussens LM. Lymphocytes in cancer development: Polarization towards pro-tumor immunity. Cytokine Growth Factor Rev. 2010; 21:3–10. [PubMed: 20005150]
13. Zou W. Regulatory T cells, tumour immunity and immunotherapy. Nat Rev Immunol. 2006; 6:295–307. [PubMed: 16557261]
14. Deeb KK, Michalowska AM, Yoon CY, Krummey SM, Hoenerhoff MJ, Kavanaugh C, Li MC, Demayo FJ, Linnoila I, Deng CX, Lee EY, Medina D, Shih JH, Green JE. Identification of an integrated SV40 T/t-antigen cancer signature in aggressive human breast, prostate, and lung carcinomas with poor prognosis. Cancer Res. 2007; 67:8065–8080. [PubMed: 17804718]
15. Magdaleno SM, Wang G, Mireles VL, Ray MK, Finegold MJ, DeMayo FJ. Cyclin-dependent kinase inhibitor expression in pulmonary Clara cells transformed with SV40 large T antigen in transgenic mice. Cell Growth Differ. 1997; 8:145–155. [PubMed: 9040936]
16. de Visser KE, Korets LV, Coussens LM. De novo carcinogenesis promoted by chronic inflammation is B lymphocyte dependent. Cancer Cell. 2005; 7:411–423. [PubMed: 15894262]
17. Andreu P, Johansson M, Affara NI, Pucci F, Tan T, Junankar S, Korets L, Lam J, Tawfik D, DeNardo DG, Naldini L, de Visser KE, De Palma M, Coussens LM. FcRgamma activation regulates inflammation-associated squamous carcinogenesis. Cancer Cell. 2010; 17:121–134. [PubMed: 20138013]
18. Ruffell B, Au A, Rugo HS, Esserman LJ, Hwang ES, Coussens LM. Leukocyte composition of human breast cancer. Proc Natl Acad Sci U S A. 2012; 109:2796–2801. [PubMed: 21825174]
19. DeNardo DG, Brennan DJ, Rexhepaj E, Ruffell B, Shiao SL, Madden SF, Gallagher WM, Wadhwani N, Keil SD, Junaid SA, Rugo HS, Hwang ES, Jirstrom K, West BL, Coussens LM.

Leukocyte complexity predicts breast cancer survival and functionally regulates response to chemotherapy. Cancer Discov. 2011; 1:54–67. [PubMed: 22039576]

20. Brunkow ME, Jeffery EW, Hjerrild KA, Paeper B, Clark LB, Yasayko SA, Wilkinson JE, Galas D, Ziegler SF, Ramsdell F. Disruption of a new forkhead/winged-helix protein, scurfin, results in the fatal lymphoproliferative disorder of the scurfy mouse. Nat Genet. 2001; 27:68–73. [PubMed: 11138001]
21. Kim J, Lahl K, Hori S, Loddenkemper C, Chaudhry A, deRoos P, Rudensky A, Sparwasser T. Cutting edge: depletion of Foxp3+ cells leads to induction of autoimmunity by specific ablation of regulatory T cells in genetically targeted mice. J Immunol. 2009; 183:7631–7634. [PubMed: 19923467]
22. Munn DH, Mellor AL. IDO and tolerance to tumors. Trends Mol Med. 2004; 10:15–18. [PubMed: 14720581]
23. Mellor AL, Munn D. Policing pregnancy: Tregs help keep the peace. Trends Immunol. 2004; 25:563–565. [PubMed: 15489182]
24. Travis MA, Reizis B, Melton AC, Masteller E, Tang Q, Proctor JM, Wang Y, Bernstein X, Huang X, Reichardt LF, Bluestone JA, Sheppard D. Loss of integrin alpha(v)beta8 on dendritic cells causes autoimmunity and colitis in mice. Nature. 2007; 449:361–365. [PubMed: 17694047]
25. Coombes JL, Siddiqui KR, Arancibia-Carcamo CV, Hall J, Sun CM, Belkaid Y, Powrie F. A functionally specialized population of mucosal CD103+ DCs induces Foxp3+ regulatory T cells via a TGF-beta and retinoic acid-dependent mechanism. J Exp Med. 2007; 204:1757–1764. [PubMed: 17620361]
26. Quezada SA, Peggs KS, Simpson TR, Shen Y, Littman DR, Allison JP. Limited tumor infiltration by activated T effector cells restricts the therapeutic activity of regulatory T cell depletion against established melanoma. J Exp Med. 2008; 205:2125–2138. [PubMed: 18725522]
27. Pegram MD, Slamon DJ. Combination therapy with trastuzumab (Herceptin) and cisplatin for chemoresistant metastatic breast cancer: evidence for receptor-enhanced chemosensitivity. Semin Oncol. 1999; 26:89–95. [PubMed: 10482199]
28. Rosell R, Robinet G, Szczesna A, Ramlau R, Constenla M, Mennecier BC, Pfeifer W, O'Byrne KJ, Welte T, Kolb R, Pirker R, Chemaissani A, Perol M, Ranson MR, Ellis PA, Pilz K, Reck M. Randomized phase II study of cetuximab plus cisplatin/vinorelbine compared with cisplatin/vinorelbine alone as first-line therapy in EGFR-expressing advanced non-small-cell lung cancer. Ann Oncol. 2008; 19:362–369. [PubMed: 17947225]
29. Koebel CM, Vermi W, Swann JB, Zerafa N, Rodig SJ, Old LJ, Smyth MJ, Schreiber RD. Adaptive immunity maintains occult cancer in an equilibrium state. Nature. 2007; 450:903–907. [PubMed: 18026089]
30. Daniel D, Chiu C, Giraudo E, Inoue M, Mizzen LA, Chu NR, Hanahan D. CD4+ T cell-mediated antigen-specific immunotherapy in a mouse model of cervical cancer. Cancer Res. 2005; 65:2018–2025. [PubMed: 15753402]
31. Girardi M, Oppenheim D, Glusac EJ, Filler R, Balmain A, Tigelaar RE, Hayday AC. Characterizing the protective component of the alphabeta T cell response to transplantable squamous cell carcinoma. J Invest Dermatol. 2004; 122:699–706. [PubMed: 15086556]
32. Daniel D, Meyer-Morse N, Bergsland EK, Dehne K, Coussens LM, Hanahan D. Immune enhancement of skin carcinogenesis by CD4+ T cells. J Exp Med. 2003; 197:1017–1028. [PubMed: 12695493]
33. Shah S, Divekar AA, Hilchey SP, Cho HM, Newman CL, Shin SU, Nechustan H, Challita-Eid PM, Segal BM, Yi KH, Rosenblatt JD. Increased rejection of primary tumors in mice lacking B cells: inhibition of anti-tumor CTL and TH1 cytokine responses by B cells. Int J Cancer. 2005; 117:574–586. [PubMed: 15912532]
34. Barbera-Guillem E, Nelson MB, Barr B, Nyhus JK, May KF Jr, Feng L, Sampsel JW. B lymphocyte pathology in human colorectal cancer. Experimental and clinical therapeutic effects of partial B cell depletion. Cancer Immunol Immunother. 2000; 48:541–549. [PubMed: 10630306]
35. Schultz KR, Klarnet JP, Gieni RS, HayGlass KT, Greenberg PD. The role of B cells for in vivo T cell responses to a Friend virus-induced leukemia. Science. 1990; 249:921–923. [PubMed: 2118273]

36. DiLillo DJ, Yanaba K, Tedder TF. B cells are required for optimal CD4+ and CD8+ T cell tumor immunity: therapeutic B cell depletion enhances B16 melanoma growth in mice. J Immunol. 184:4006–4016. [PubMed: 20194720]
37. Schneider T, Kimpfler S, Warth A, Schnabel PA, Dienemann H, Schadendorf D, Hoffmann H, Umansky V. Foxp3(+) regulatory T cells and natural killer cells distinctly infiltrate primary tumors and draining lymph nodes in pulmonary adenocarcinoma. J Thorac Oncol. 6:432–438. [PubMed: 21258248]
38. Dimitrakopoulos FI, Papadaki H, Antonacopoulou AG, Kottorou A, Gotsis AD, Scopa C, Kalofonos HP, Mouzaki A. Association of FOXP3 Expression with Non-small Cell Lung Cancer. Anticancer Res. 31:1677–1683. [PubMed: 21617226]
39. Sun JC, Williams MA, Bevan MJ. CD4+ T cells are required for the maintenance, not programming, of memory CD8+ T cells after acute infection. Nat Immunol. 2004; 5:927–933. [PubMed: 15300249]
40. Shedlock H. Requirement for CD4 T cell help in generating functional CD8 T cell memory. Science. 2003; 300:337–339. [PubMed: 12690201]
41. Onizuka S, Tawara I, Shimizu J, Sakaguchi S, Fujita T, Nakayama E. Tumor rejection by in vivo administration of anti-CD25 (interleukin-2 receptor alpha) monoclonal antibody. Cancer Res. 1999; 59:3128–3133. [PubMed: 10397255]
42. Shimizu J, Yamazaki S, Sakaguchi S. Induction of tumor immunity by removing CD25+CD4+ T cells: a common basis between tumor immunity and autoimmunity. J Immunol. 1999; 163:5211–5218. [PubMed: 10553041]
43. Golgher D, Jones E, Powrie F, Elliott T, Gallimore A. Depletion of CD25+ regulatory cells uncovers immune responses to shared murine tumor rejection antigens. Eur J Immunol. 2002; 32:3267–3275. [PubMed: 12555672]
44. Casares N, Arribillaga L, Sarobe P, Dotor J, Lopez-Diaz de, Cerio A, Melero I, Prieto J, Borras-Cuesta F, Lasarte JJ. CD4+/CD25+ regulatory cells inhibit activation of tumor-primed CD4+ T cells with IFN-gamma-dependent antiangiogenic activity, as well as long-lasting tumor immunity elicited by peptide vaccination. J Immunol. 2003; 171:5931–5939. [PubMed: 14634104]
45. Jones E, Dahm-Vicker M, Simon AK, Green A, Powrie F, Cerundolo V, Gallimore A. Depletion of CD25+ regulatory cells results in suppression of melanoma growth and induction of autoreactivity in mice. Cancer Immun. 2002; 2:1. [PubMed: 12747746]
46. Beyer M, Schultze JL. Regulatory T cells in cancer. Blood. 2006; 108:804–811. [PubMed: 16861339]
47. Ghiringhelli F, Menard C, Terme M, Flament C, Taieb J, Chaput N, Puig PE, Novault S, Escudier B, Vivier E, Lecesne A, Robert C, Blay JY, Bernard J, Caillat-Zucman S, Freitas A, Tursz T, Wagner-Ballon O, Capron C, Vainchencker W, Martin F, Zitvogel L. CD4+CD25+ regulatory T cells inhibit natural killer cell functions in a transforming growth factor-beta-dependent manner. J Exp Med. 2005; 202:1075–1085. [PubMed: 16230475]
48. Teng MW, Swann JB, von Scheidt B, Sharkey J, Zerafa N, McLaughlin N, Yamaguchi T, Sakaguchi S, Darcy PK, Smyth MJ. Multiple antitumor mechanisms downstream of prophylactic regulatory T-cell depletion. Cancer Res. 70:2665–2674. [PubMed: 20332236]
49. Tadokoro CE, Shakhar G, Shen S, Ding Y, Lino AC, Maraver A, Lafaille JJ, Dustin ML. Regulatory T cells inhibit stable contacts between CD4+ T cells and dendritic cells in vivo. J Exp Med. 2006; 203:505–511. [PubMed: 16533880]
50. Mahajan D, Wang Y, Qin X, Zheng G, Wang YM, Alexander SI, Harris DC. CD4+CD25+ regulatory T cells protect against injury in an innate murine model of chronic kidney disease. J Am Soc Nephrol. 2006; 17:2731–2741. [PubMed: 16988067]
51. Tiemessen MM, Jagger AL, Evans HG, van Herwijnen MJ, John S, Taams LS. CD4+CD25+Foxp3+ regulatory T cells induce alternative activation of human monocytes/macrophages. Proc Natl Acad Sci U S A. 2007; 104:19446–19451. [PubMed: 18042719]
52. Zhen Y, Zheng J, Zhao Y. Regulatory CD4+CD25+ T cells and macrophages: communication between two regulators of effector T cells. Inflamm Res. 2008; 57:564–570. [PubMed: 19109736]
53. Tawara I, Take Y, Uenaka A, Noguchi Y, Nakayama E. Sequential involvement of two distinct CD4+ regulatory T cells during the course of transplantable tumor growth and protection from 3-

methylcholanthrene-induced tumorigenesis by CD25-depletion. Jpn J Cancer Res. 2002; 93:911–916. [PubMed: 12716469]

54. Yu P, Lee Y, Liu W, Krausz T, Chong A, Schreiber H, Fu YX. Intratumor depletion of CD4+ cells unmasks tumor immunogenicity leading to the rejection of late-stage tumors. J Exp Med. 2005; 201:779–791. [PubMed: 15753211]
55. Zitvogel L, Apetoh L, Ghiringhelli F, Kroemer G. Immunological aspects of cancer chemotherapy. Nat Rev Immunol. 2008; 8:59–73. [PubMed: 18097448]
56. Anraku M, Tagawa T, Wu L, Yun Z, Keshavjee S, Zhang L, Johnston MR, de Perrot M. Synergistic antitumor effects of regulatory T cell blockade combined with pemetrexed in murine malignant mesothelioma. J Immunol. 2010; 185:956–966. [PubMed: 20548032]
57. Teng MW, Ngiow SF, von Scheidt B, McLaughlin N, Sparwasser T, Smyth MJ. Conditional regulatory T-cell depletion releases adaptive immunity preventing carcinogenesis and suppressing established tumor growth. Cancer Res. 2010; 70:7800–7809. [PubMed: 20924111]
58. Klages K, Mayer CT, Lahl K, Loddenkemper C, Teng MW, Ngiow SF, Smyth MJ, Hamann A, Huehn J, Sparwasser T. Selective depletion of Foxp3+ regulatory T cells improves effective therapeutic vaccination against established melanoma. Cancer Res. 2010; 70:7788–7799. [PubMed: 20924102]
59. Malchow S, Leventhal DS, Nishi S, Fischer BI, Shen L, Paner GP, Amit AS, Kang C, Geddes JE, Allison JP, Socci ND, Savage PA. Aire-dependent thymic development of tumor-associated regulatory T cells. Science. 2013; 339:1219–1224. [PubMed: 23471412]

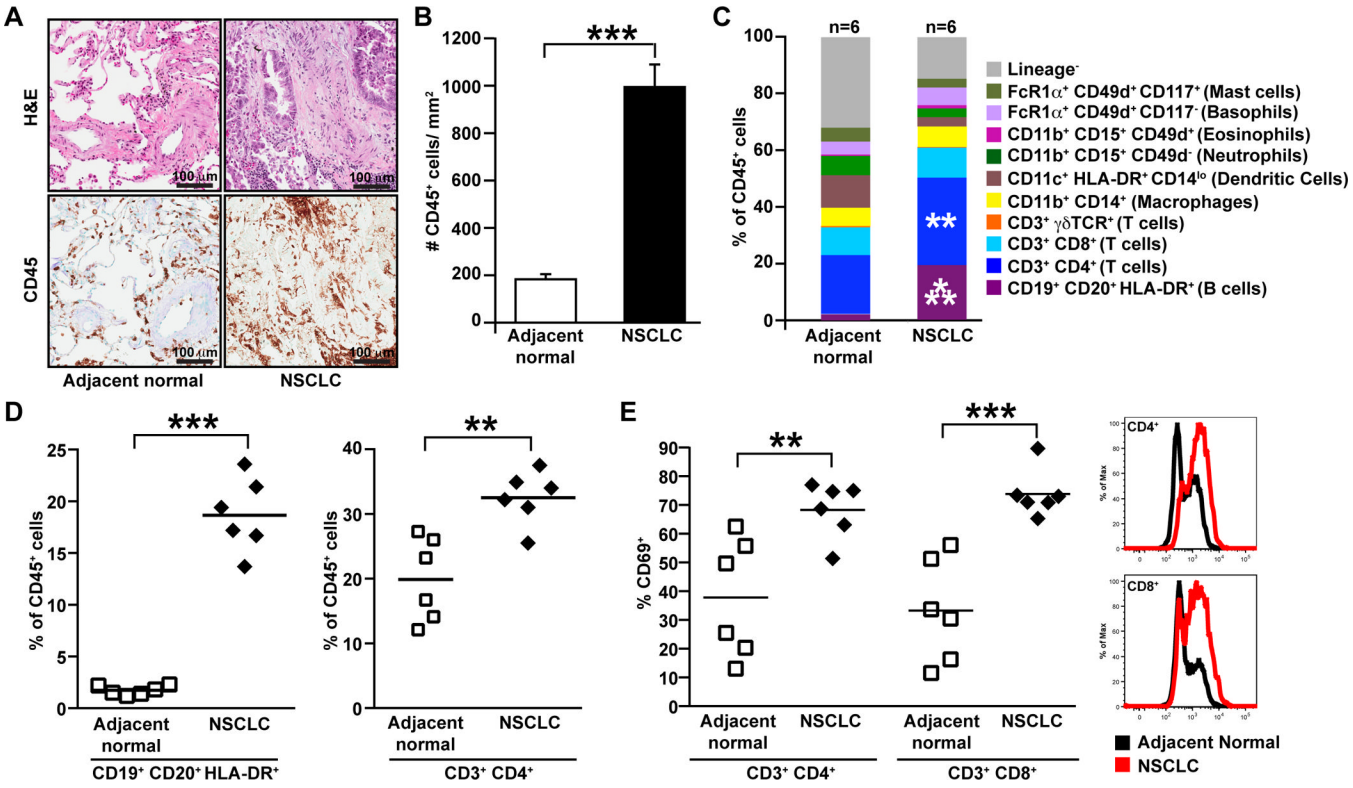

Figure 1. Immune complexity of human NSCLC

(A) Hematoxylin and eosin (H&E) staining of human non-small cell lung cancer (NSCLC) and adjacent normal tissue (top panel) with representative images showing staining for CD45 (bottom panel). (B) Numbers of $CD45^+$ leukocytes per square millimeter of tissue sections as assessed immunohistochemistry. n=8 samples per group. (C) Flow cytometric analysis of immune cell infiltrates within human NSCLC represented as percentage of total $CD45^+$ leukocytes. n=6 samples per group. (D) $CD19^+CD20^+HLA\text{-}DR^+$ B cell and $CD3^+CD4^+$ T cell infiltrate within human NSCLC as assessed by flow cytometry, shown as a percent of total $CD45^+$ cells. (E) Percent of $CD4^+$ and $CD8^+$ T cells staining positive for CD69 as assessed by flow cytometry, with representative histograms of CD69 expression shown to the right. *p<0.05; **p<0.01, ***p<0.001.

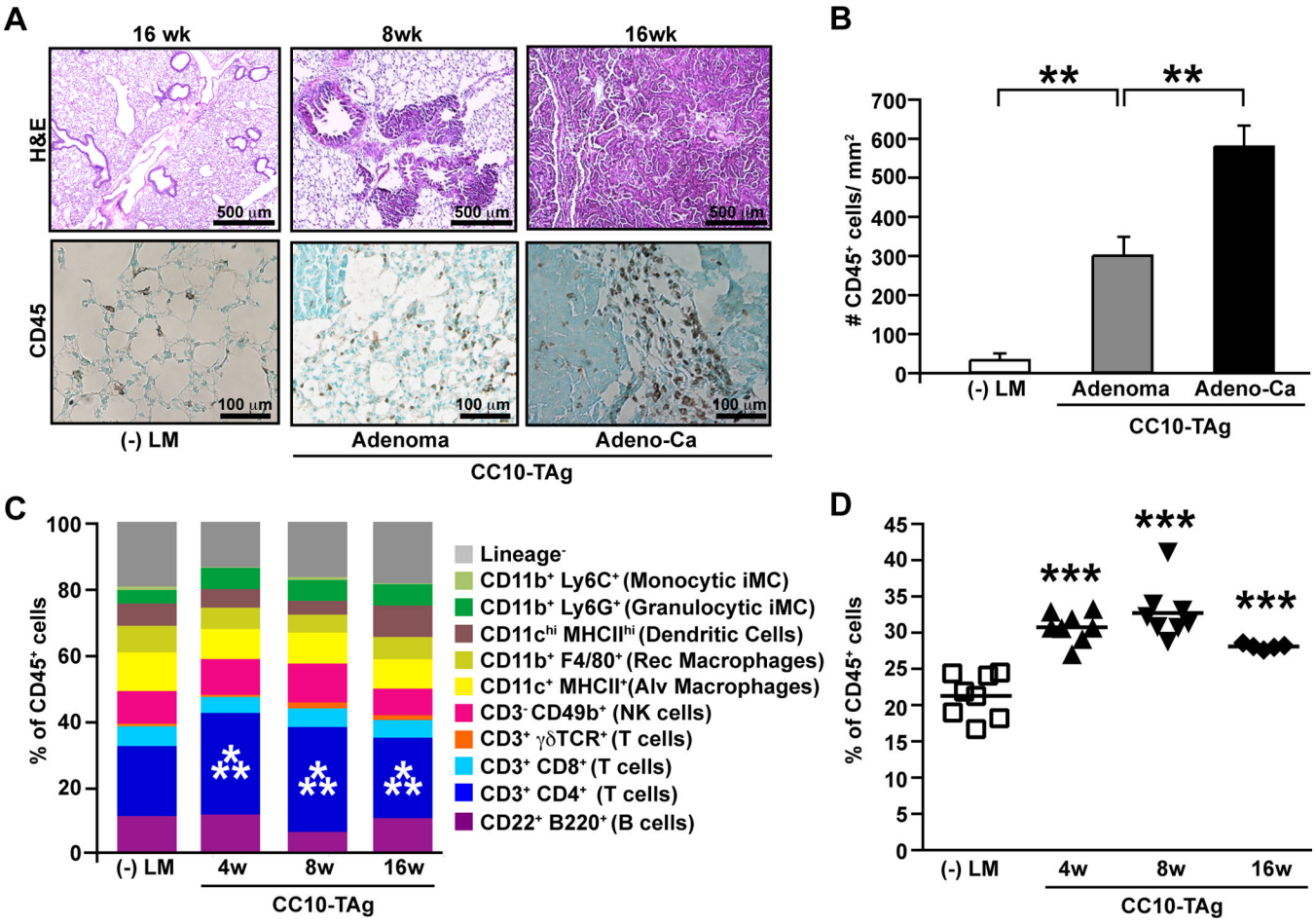

Figure 2. Immune complexity of NSCLC in CC10-TAg mice

(A) H&E staining of lungs from negative littermates (-LM) and CC10-TAg mice showing adenomas and adenocarcinoma (top panel), with representative staining for CD45 (bottom panel). (B) Numbers of $CD45^+$ leukocytes per square millimeter of tissue as assessed by immunohistochemistry. n=5 mice per group. (C) Flow cytometric analysis of immune cell infiltrates in CC10-TAg lungs assessed at various stages of neoplastic development, namely hyperplasia/dysplasia (4 weeks), adenomas (8 weeks) and adenocarcinomas (16 weeks), represented as percentages of total $CD45^+$ leukocytes. (D) $CD4^+$ T cell lung infiltrate as assessed by flow cytometry, shown as a percent of total $CD45^+$ cells. n=5∓8 mice per group. Significant differences are shown relative to negative littermates. *p<0.05; **p<0.01, ***p<0.001.

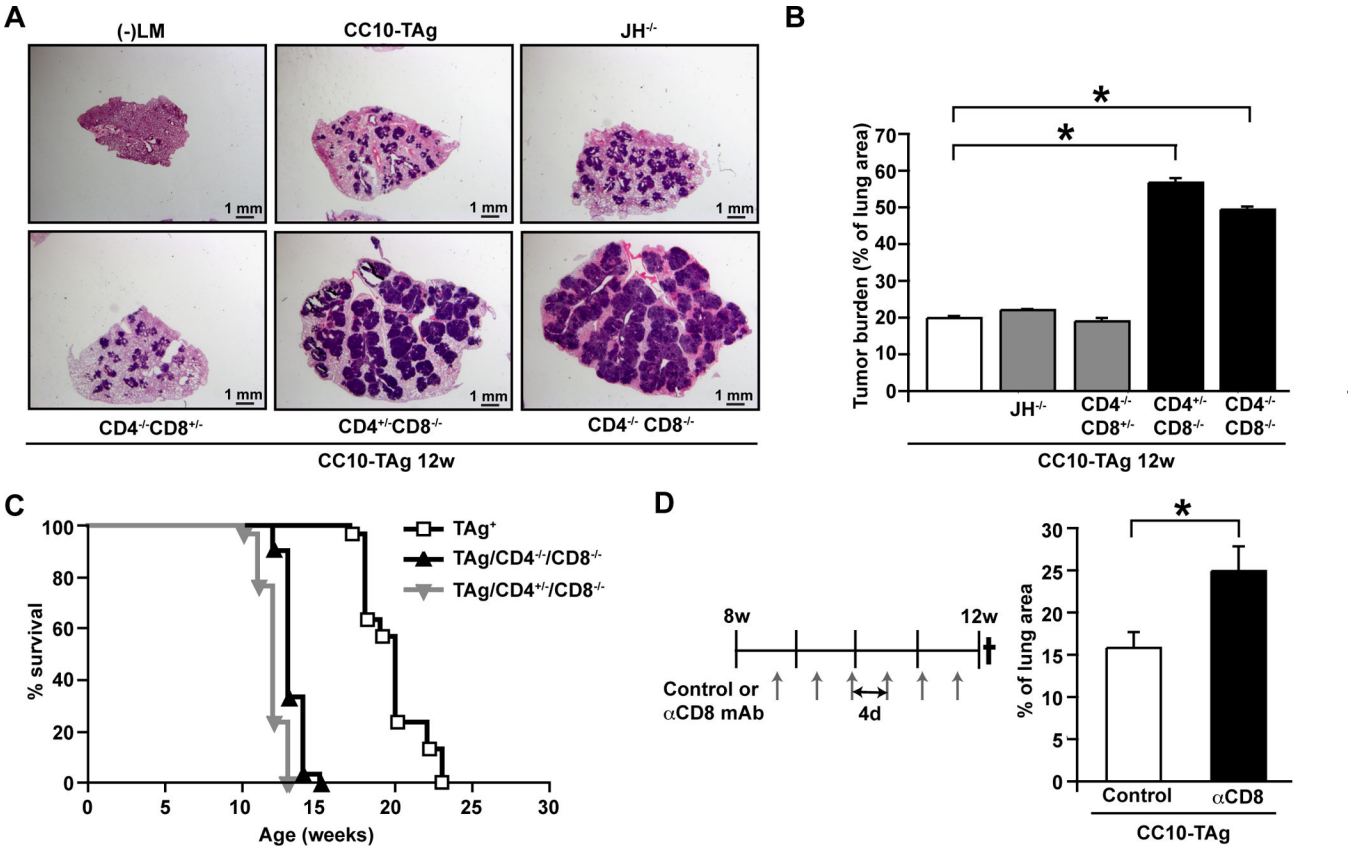

Figure 3. CD8$^+$ T cells restrain NSCLC growth in CC10-TAg mice

(A) H&E staining of lungs from CC10-TAg mice deficient for selective lymphocyte subsets. (B) Quantification of tumor burden from mice shown in A. n=4∓5 mice per group. (C) Survival of CC10-TAg mice compared with those deficient in CD8$^+$ T lymphocytes. p<0.0001; n=30 mice per group. (D) Tumor burden quantified as percentage of lung area in CC10-TAg mice following CD8$^+$ T cell depletion from 8 weeks until 12 weeks of age. n=3∓7 mice per group, with one of three representative experiments shown. *p<0.05; **p<0.01, ***p<0.001.

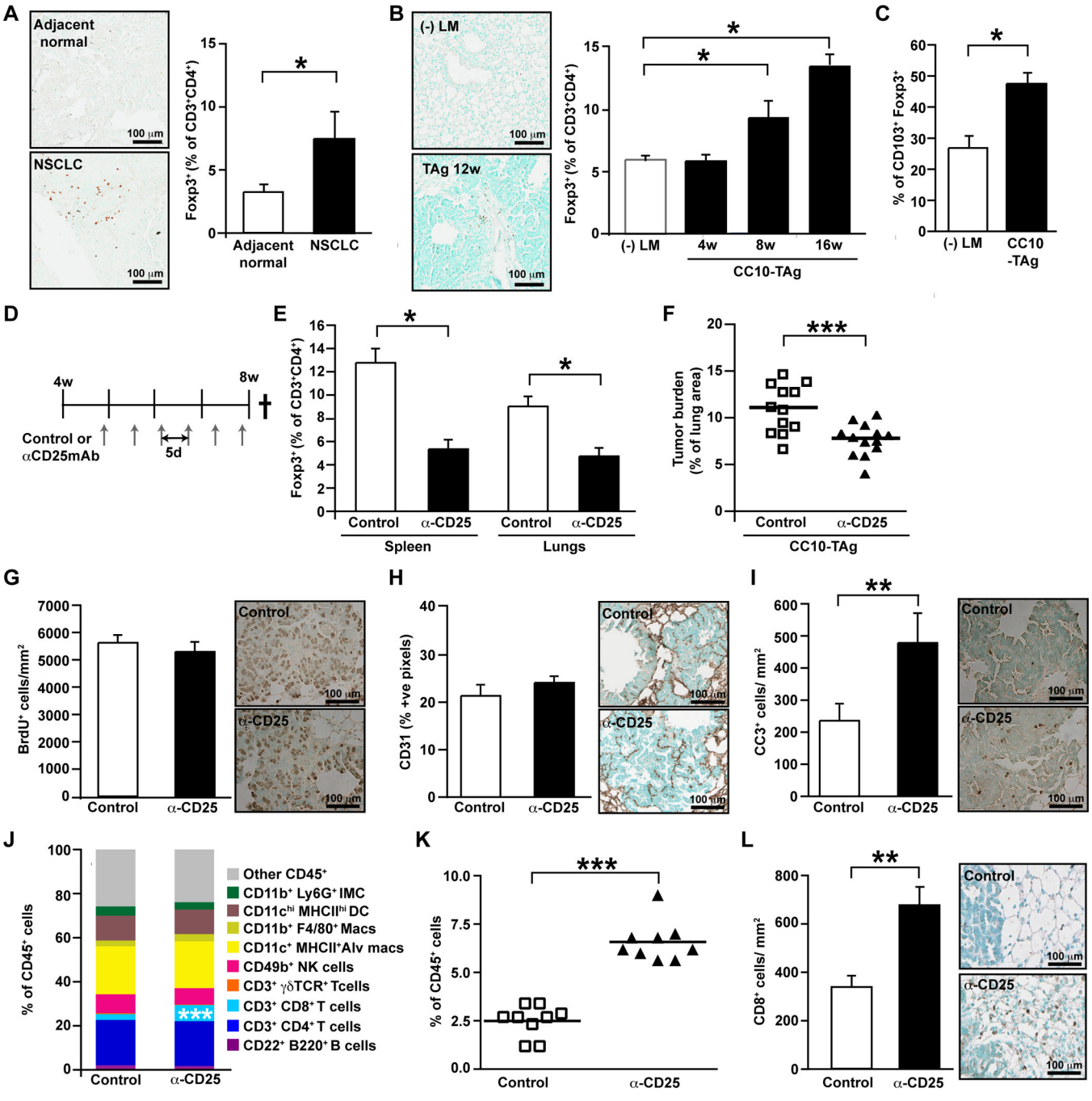

Figure 4. Functional significance of T regulatory cells in NSCLC

(A) Frequency of Foxp3$^+$ T_{reg} cells within the CD4$^+$ T cell compartment in human NSCLC assessed by flow cytometry, with representative FoxP3 immunohistochemistry shown on left. n=6 per group. (B) Frequency of Foxp3$^+$ Treg cells within the CD4$^+$ T cell compartment in CC10-TAg tumors at various ages as assessed by flow cytometry, with representative FoxP3 immunohistochemistry shown on left. n=5∓8 mice per group. (C) Percent of CD3$^+$CD4$^+$FoxP3$^+$ cells expressing CD103$^+$ in CC10-TAg tumors. n=5∓8 mice per group. (D) T_{reg} depletion was assessed in CC10-TAg mice in a prevention trial by IP injections of αCD25 mAb every 5 days from 4 weeks until 8 weeks of age. (E) Frequency of Foxp3$^+$ T_{regs} represented as percentage of CD3$^+$CD4$^+$ T cells in spleen (left) and lung

tumors (right) following treatment with αCD25 mAb. (F) Tumor burden represented as percentage of lung area following αCD25 treatment in CC10-TAg mice. (G) Number of $BrdU^+$ tumor cells per square millimeter of lung tumors. (H) Angiogenic vasculature represented as percent positive pixels of CD31 staining by automated quantification of representative stained sections. (I) Number of cleaved caspase 3^+ tumor cells per square millimeter of lung tumors. (J) Immune cell complexity of lung tumors following T_{reg} depletion represented as percentage of $CD45^+$ leukocytes assessed by flow cytometry. (K) $CD8^+$ T cell infiltrate of lung tumors as assessed by flow cytometry, shown as a percent of total $CD45^+$ cells. (L) Absolute numbers of $CD8^+$ cells per square millimeter of lung tumor with representative immunohistochemistry shown to the right. (E-L) n=12∓13 mice per group with data obtained over 3 independent cohorts of animals. *p<0.05; **p<0.01, ***p<0.001.

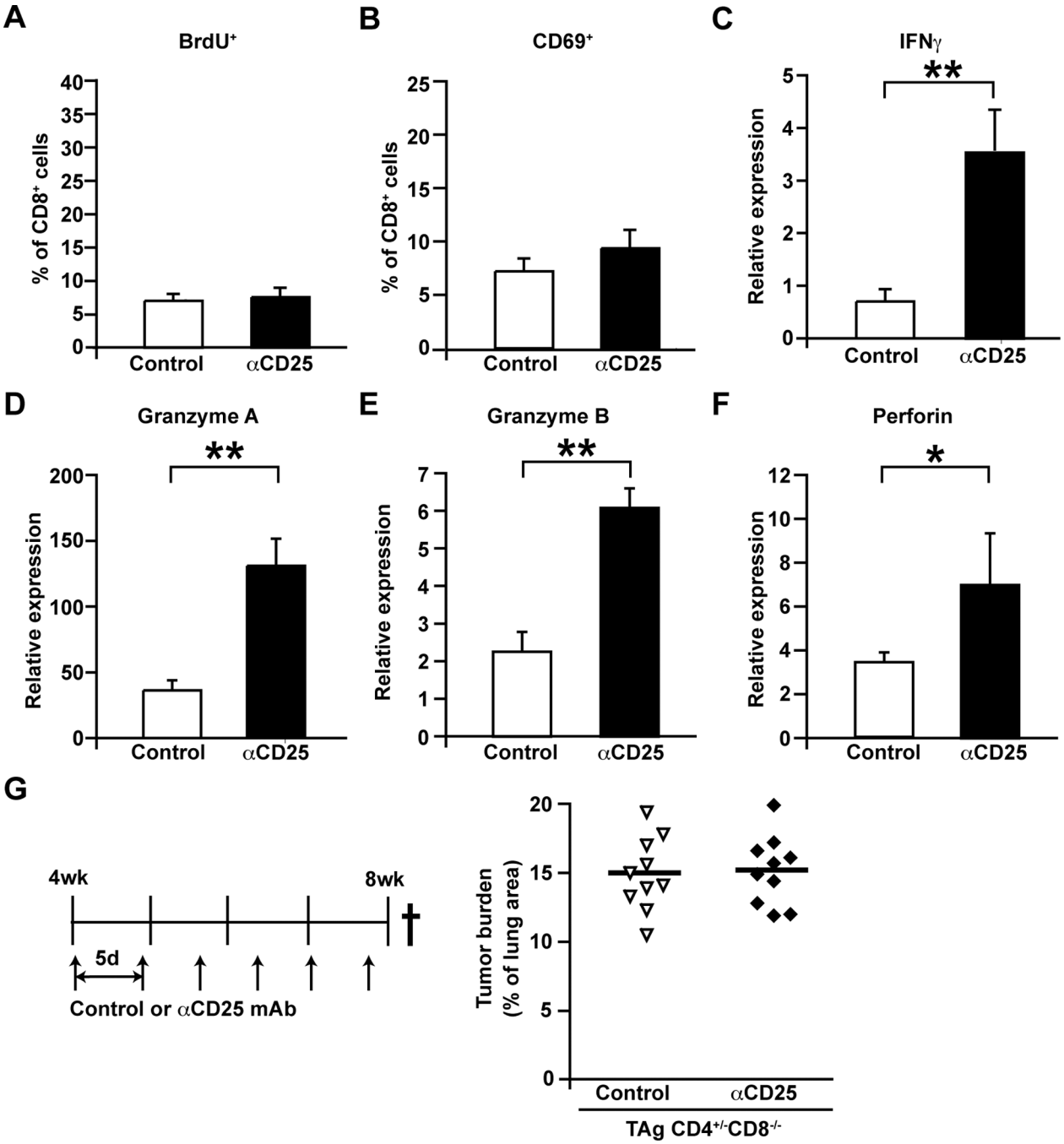

Figure 5. CD8$^+$ T cells in NSCLC following T$_{reg}$ depletion

(A) Frequency of BrdU$^+$ proliferating CD8$^+$ T cells represented as percentages of total tumor infiltrating CD8$^+$ T cells. (B) Frequency of CD69-expressing activated CD8$^+$ T cells represented as percentages of total tumor infiltrating CD8+ T cells. (A-B) n=7 per group, one of two representative experiments is shown. (C-F) Relative expression of *Ifng* (C), *Gzma* (D) *Gzmb* (E) and *Prf1* (F) mRNA in flow-sorted CD8$^+$ T cells represented as fold change over *Tbp* as assessed by qPCR. n=7 per group, with data obtained over 2 independent cohorts of animals. (G) Tumor burden represented as percentage of lung area, following treatment with αCD25 mAb from 4 weeks until 8 weeks of age in CC10-TAg

mice deficient in $CD8^+$ T cells. n=10 per group, with data obtained over 3 independent cohorts of animals. *p<0.05; **p<0.01, ***p<0.001.

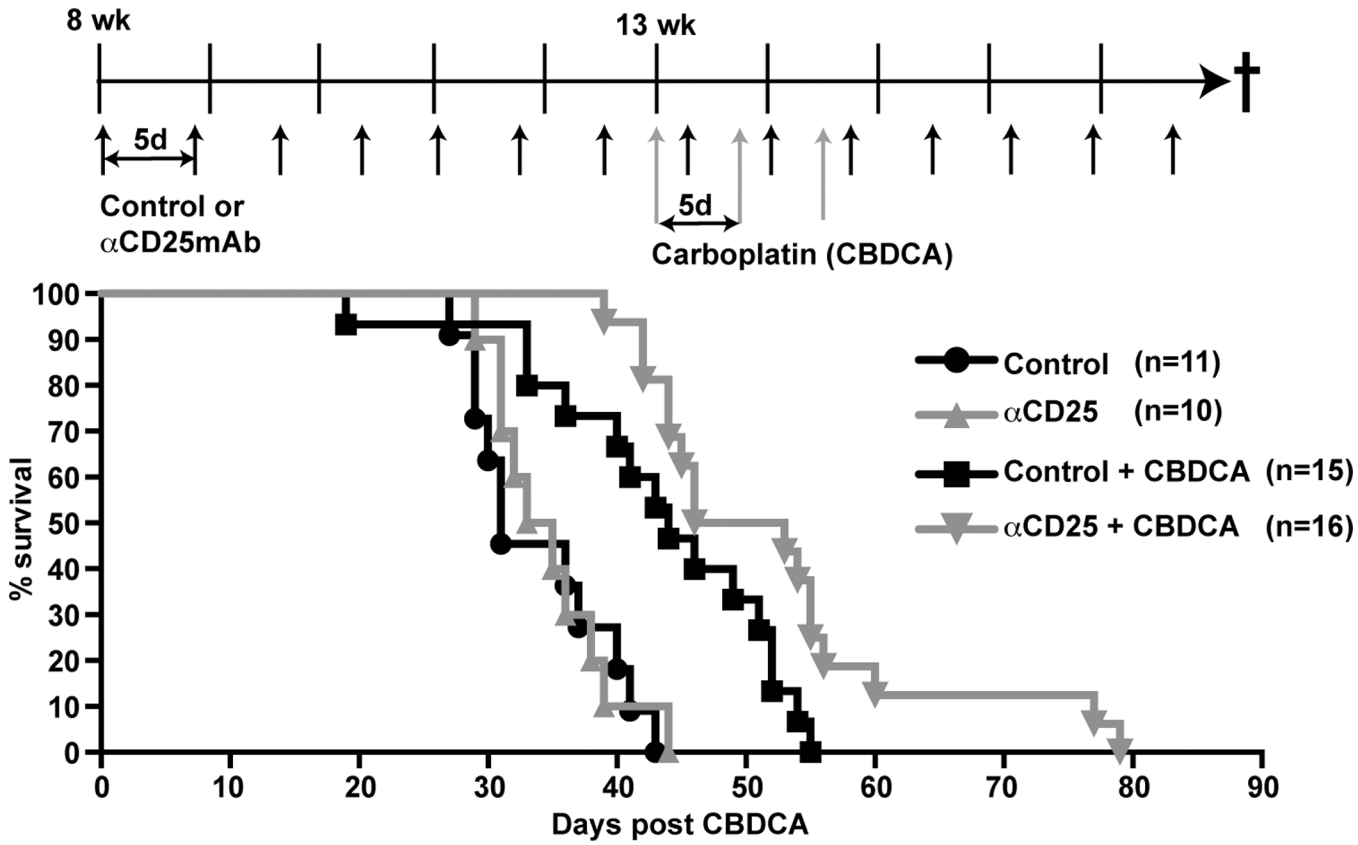

Figure 6. T regulatory cell depletion in combination with chemotherapy extends survival

Percent survival of CC10-TAg mice treated with control IgG or αCD25 mAb as monotherapy, or in combination with 50 mg/kg carboplatin (CBDCA). Dosing strategy is shown above the survival graph. Mice received control IgG or αCD25 mAb from 8 weeks of age until end-stage determined by 15% weight loss. Carboplatin was administered in 3 doses, 5 days apart, commencing at 13 weeks. Over 15 cohorts of mice were treated to obtain 10∓16 mice per group. $p<0.05$, control versus CBDCA alone; $p<0.05$, CBDCA alone versus αCD25/CBDCA.